

## Effect of midblock on the morphology and properties of blends of ABA triblock copolymers of PDLA-mid-block-PDLA with PLLA

Sahas R. Rathi<sup>a</sup>, E. Bryan Coughlin<sup>a,\*\*</sup>, Shaw Ling Hsu<sup>a,\*</sup>, Charles S. Golub<sup>b</sup>, Gerald H. Ling<sup>b</sup>, Michael J. Tzivanis<sup>b</sup>

<sup>a</sup> Polymer Science and Engineering, University of Massachusetts, Amherst, MA 01003, USA

<sup>b</sup> Saint Gobain Fluid Systems, Research & Development Center, 9 Goddard Road, Northborough, MA 01532, USA

### ARTICLE INFO

#### Article history:

Received 28 December 2011

Received in revised form

1 May 2012

Accepted 6 May 2012

Available online 14 May 2012

#### Keywords:

PLA

Toughen

Stereocomplex

### ABSTRACT

A method to overcome the brittleness of poly(L-lactic acid) (PLLA) by kinetically trapping a continuous low  $T_g$  amorphous phase is presented. This morphology is accomplished by exploiting the significant difference in the crystallization temperatures of PLLA vs its stereocomplex with the poly(D-lactic acid) (PDLA) isomer. In our studies, the D isomer is the end block of a triblock copolymer with a configuration of the form PDLA<sub>n</sub>–Soft Block<sub>m</sub>–PDLA<sub>n</sub>. As demonstrated in this study, when blended with PLLA, the obtained morphology, and improvement in the sample toughness and flexibility, strongly depend on the miscibility of the midblock in the triblock copolymer with the matrix PLLA. The difference in the chemical nature of the midblock clearly affected the stereocomplex crystallization between the PDLA end blocks, the PLLA matrix polymer, and the morphology formed. It is found that the miscible midblock gives rise to a soft continuous amorphous phase while in the case of an immiscible midblock, a glassy phase separated amorphous phase is formed. Dramatically different physical properties can be obtained for various PLLA/triblock copolymer blends giving access to tough, yet flexible, semicrystalline PLLA blends.

© 2012 Elsevier Ltd. All rights reserved.

### 1. Introduction

The extremely rapid crystallization kinetics of poly(L-lactic acid) (PLLA) when deformed, result in a high degree of crystallinity making it brittle in nature [1]. If the crystallization of PLLA can be arrested, and the remaining polymer trapped in a continuous amorphous phase, then the brittleness associated with these materials can be reduced. Moreover, if the continuous amorphous phase is in the rubbery state at ambient conditions, a tough flexible semicrystalline material may be obtained. Our previous work introduced a concept for toughening semicrystalline poly(lactic acid) based on this hypothesis [2]. This concept was developed using a stereocomplex forming triblock copolymer with a general structure PDLA<sub>n</sub>–mid-block<sub>m</sub>–PDLA<sub>n</sub> as a combination of nucleating agent, compatibilizer, and softening agent for PLLA. These PLLA/triblock copolymer blends form a morphology which can be described as stereocomplex crystallites serving as nano-reinforcements dispersed in a continuous amorphous phase matrix.

In our previous study [2] we had proposed four possible toughening mechanisms when polyethylene glycol (PEG) was the midblock in the triblock copolymer/PLLA blends. These possibilities are: 1) Softening of the amorphous phase due to lowering of the glass transition temperature. 2) The existence of a continuous amorphous phase. 3) The presence of a soft dispersed amorphous soft block-rich phase within the amorphous regions of the crystalline lamellae. 4) The presence of the  $\alpha'$  phase of PLLA. Our initial study has shown that a flexible continuous amorphous phase (combining possibilities #1 and #2) is a necessary component. A low  $T_g$  amorphous phase will have elevated chain mobility at ambient conditions to absorb and dissipate applied stress and is an attractive morphology to obtain tough materials [2–4]. Although our intuitive notion proved to be successful, the effect of the chemical nature of the midblock on the morphology development has not been investigated. One of the most intriguing aspects is the miscibility between the soft midblock and PLLA, and the variation in the morphological features obtained. If the midblock is miscible with PLLA, a homogenous, soft, continuous amorphous phase can be formed. It is formed due to the molecular scale dispersion of the free fraction of the triblock copolymer in the PLLA matrix. The  $T_g$  of a miscible blend is intermediate between the values for each component [5]. On the other hand, an immiscible midblock will lead to the formation of phase separated domains of the triblock

\* Corresponding author. Tel.: +1 413 577 1411.

\*\* Corresponding author. Tel.: +1 413 577 1616.

E-mail addresses: [coughlin@mail.pse.umass.edu](mailto:coughlin@mail.pse.umass.edu) (E.B. Coughlin), [slhsu@polysci.umass.edu](mailto:slhsu@polysci.umass.edu) (S.L. Hsu).

copolymer, giving a morphology similar to more traditional rubber toughened systems [6]. The nature of the midblock also controls the proximity of the end blocks (PDLA) and the matrix polymer (PLLA), thus forming a different amorphous phase, possessing different physical properties.

The two soft blocks chosen for this study are poly(ethylene glycol-propylene glycol) (PEPG), a polymer miscible with PLA, and poly(ethylene-butylene) copolymer (EB), a polymer immiscible with PLA. The two soft blocks have similar  $T_g$  values (approximately  $-60^\circ\text{C}$ ) thus making them physically similar but chemically different. The Flory–Huggins interaction parameter ( $\chi$ ) between PLA and poly(ethylene glycol) (PEG) is 0.0, 0.5 for PLA/PEG200 and PLA/PEG1000 blends, respectively [3]. The solubility parameter for PEG does not vary appreciably with molecular weight [7]. In fact, previous studies indicate that PEG/PLA will form miscible blends. Copolymerization of ethylene glycol with propylene glycol forms poly(ethylene glycol-propylene glycol) (PEPG). Previous studies have also shown that this copolymer has similar plasticization efficiency as PEG, with the added advantage of being amorphous at ambient conditions. This makes these blends more stable than PLA/PEG blends [8,9]. To study the other extreme, a poly(ethylene-butylene) copolymer system, being extremely hydrophobic and immiscible with PLLA, was chosen. A comparison of the morphologies formed and the resultant mechanical properties are reported here.

## 2. Experimental

### 2.1. Materials

D-Lactide ((3R-cis)-3,6-dimethyl-1,4-dioxane-2,5-dione) was obtained from Purac Biochem BV (Gorinchem, The Netherlands) and recrystallized from toluene before use. PLLA (4.2%D) (PLA2002D) was obtained from Natureworks. Stannous octoate (tin(II) bis(2-ethylhexanoate),  $\text{Sn}(\text{Oct})_2$ , 96%) was purchased from Sigma Chemical Co. and was used as-received. PEPG12000 (UCON Lubricant 75-H-90000; functionality 2,  $\bar{D}$ : 1.10) was obtained from Dow Chemicals, USA. The PEPG12k has a  $T_g$  of  $-68^\circ\text{C}$  and a melting point of  $-2^\circ\text{C}$ . Hydroxyl-terminated linear butadiene, with a minor proportion (<8%) of monohydroxyl terminated and polybutadiene without hydroxyl groups (LBH10k) (average functionality 1.9, vinyl content 65 wt%) was obtained from Crayvalley, USA. The LBH10k had a  $T_g$  of  $-55^\circ\text{C}$ . Poly(ethylene-butylene) copolymer (EB) was obtained by hydrogenation of the LBH10k polymer and had a  $T_g$  of  $-60^\circ\text{C}$ .

### 2.2. Triblock synthesis

The triblock copolymers were synthesized by ring-opening polymerization (ROP) of D-lactide using the hydroxyl-terminated soft block as an initiator and stannous octoate as a catalyst. Depending on the miscibility of the midblock with PDLA either solution polymerization or bulk polymerization conditions were used to synthesize the triblock copolymers. The two triblock copolymers synthesized are PDLA40-PEPG12k-PDLA40 and PDLA60-EB10k-PDLA60. The nomenclature used is PDLAn-SoftBlockm-PDLAn, where n stands for the degree of polymerization of PDLA with lactic acid as a repeat unit and m stands for the number average molecular weight of the soft midblock. For example 12k stands for 12,000 g/mol.

### 2.3. Poly(ethyleneglycol-random-propylene glycol) (PEPG) midblock

The required amount of PEPG12000 was placed in a flame dried Schlenk flask and subjected to azeotropic distillation with toluene. D-Lactide was then added under a nitrogen atmosphere and the

flask was placed in an oil bath maintained at  $130^\circ\text{C}$ . After 15 min, the required amount of stannous octoate in  $\sim 0.5$  ml toluene was injected into the flask. At the end of 6 h of reaction time the polymer obtained was dissolved in dichloromethane, precipitated in diethyl ether and dried in vacuo. The reaction was conducted on a 60 g scale.

### 2.4. Poly(ethylene-butylene) (EB) midblock

The reaction steps involved in the synthesis of poly(ethylene-butylene) based triblock copolymer are as follows: the as-received polymer (LBH10k) was hydrogenated to obtain poly(ethylene-butylene) copolymer (EB10k) in order to prevent undesired side reactions during the subsequent processing steps. Hydrogenation was performed in a high pressure hydrogenation reactor on a 10 wt% Pd on activated charcoal solution of the polymer using 10 wt% Pd on activated charcoal as the catalyst at  $\sim 100^\circ\text{C}$  and 120 psi hydrogen pressure for 12 h. The poly(ethylene-butylene) copolymer was then transferred to a flame dried Schlenk flask and subjected to azeotropic distillation with toluene. D-Lactide was then added to the flask under nitrogen followed by the addition of toluene (three times the amount of reactants). The flask was then immersed in an oil bath maintained at  $110^\circ\text{C}$  and the required amount of stannous octoate in  $\sim 1$  ml toluene was injected into the flask. After 24 h the reaction was stopped, and the polymer was obtained by precipitation in excess methanol followed by drying in vacuo.

### 2.5. Blends used and evaluation of tensile properties

Blends were prepared by using a 15 cc DSM twin screw mini-extruder. The triblock copolymer and PLA 2002D were introduced into the extruder and mixed for 5 min at  $190^\circ\text{C}$  and 100 rpm. Dog-bone samples for tensile testing were obtained using a 10 cc DSM mini-injection mold. The pressure used was variable depending on viscosity. For low viscosity blends 3 bar injection pressure was used while, for higher viscosity 7 bar was used. The viscosity was inversely proportional to the amount of triblock in the blend. The mold was maintained at  $30^\circ\text{C}$  for 2 min.

Tensile testing was performed using an Instron universal testing machine according to ASTM D638 standard for tensile testing, using type IV dog bones specimens. Testing was performed at a crosshead speed of 50.8 mm/min with a 5 kN load cell. For each sample, three individual specimens were tested in separate analyses, and the data reported is the calculated means.

### 2.6. Techniques used

$^1\text{H}$  nuclear magnetic resonance (NMR) (300 MHz) spectra were obtained using a Bruker DPX-300 NMR spectrometer. The spectra were measured in  $\text{CDCl}_3$ , and the chemical shifts were calibrated to the solvents' residual proton signal ( $^1\text{H}$  NMR signal:  $\delta$  7.26 ppm for  $\text{CHCl}_3$ ). The molecular weight and dispersity were determined by GPC (chloroform) (Agilent). The molecular weights measured were with respect to polystyrene standards. Thermal characterization was performed on a TA Q100 differential scanning calorimeter (DSC) (TA Instruments) which was calibrated against an indium standard. The samples (5–10 mg) were heated at the rate of  $20^\circ\text{C min}^{-1}$  in the first cycle to study the morphology of the samples formed under the processing conditions, cooled at  $20^\circ\text{C min}^{-1}$ . In order to study the blend crystallization in greater detail, we employed a slower heating rate of  $10^\circ\text{C min}^{-1}$  in the second cycle. Microstructure analysis was performed using infrared (IR) and Raman spectroscopy. The infrared spectra were obtained by using a PerkinElmer 100 FTIR spectrometer. 32 scans were co-

added in order to achieve an acceptable signal-to-noise ratio. In all cases, spectral resolution was maintained at  $4\text{ cm}^{-1}$ . Raman spectra were obtained using a Jobin Yvon Horiba LabRam HR 800 Raman microscope. Spherulite/dendrite growth in the blends was observed using an Olympus (Tokyo, Japan) Polarized Optical Microscope (BH-2) equipped with a heating stage. The samples for optical observation were prepared by the following procedure. First a sample of  $\sim 5\text{ mg}$  was placed between a glass slide and a Kapton film, and was heated to melt completely; it was then pressed to obtain a thin film and then cooled down to room temperature. Subsequently, the sample was again melted and transferred to a hot stage which was maintained at  $155\text{ }^\circ\text{C}$ . All crystallization experiments were followed using the birefringence developed for samples between two polarizers with an orthogonal polarization axis. Images were taken with a digital camera.

### 3. Results and discussion

#### 3.1. Triblock synthesis

##### 3.1.1. PEPG midblock

The  $^1\text{H}$  NMR spectra of the PDLA40–PEPG12k–PDLA40 triblock copolymer is shown in Fig. 1. The degree of polymerization (DP) was calculated using integrated values for the methyl protons ( $-\text{CH}_3$  doublet,  $\delta \sim 1.15\text{ ppm}$ ) from the PPG unit in the PEPG midblock relative to the lactide repeat unit methine protons ( $-\text{CH}$  quartet,  $\delta \sim 5.16\text{ ppm}$ ). It was found to be in excellent agreement with the theoretical value. The dispersity determined from the GPC was 1.10 before and after polymerization indicating excellent control over the reaction. The molecular weights with respect to PS standards were  $30,500\text{ g/mol}$  and  $39,000\text{ g/mol}$  before and after polymerization respectively.

##### 3.2. Poly(ethylene–butylene) midblock

Fig. 2 shows the  $^1\text{H}$  NMR spectra of LBH10k, EB10k and PDLA60–EB10k–PDLA60 triblock copolymer. In the as-received LBH10k the resonances centered at  $\delta 1.2, 2.2, 4.8,$  and  $5.5\text{ ppm}$  are due to backbone methylene, methine, vinyl ( $\text{CH}_2$ ), vinyl ( $\text{CH}$ ) protons, respectively, from the 1,2 vinyl repeat unit. Resonances centered at  $\delta 5.35$  and  $2.00\text{ ppm}$  arise from the vinyl and methylene protons from the 1,4 repeat unit. After the hydrogenation, the downfield resonances diminish and upfield resonances increase

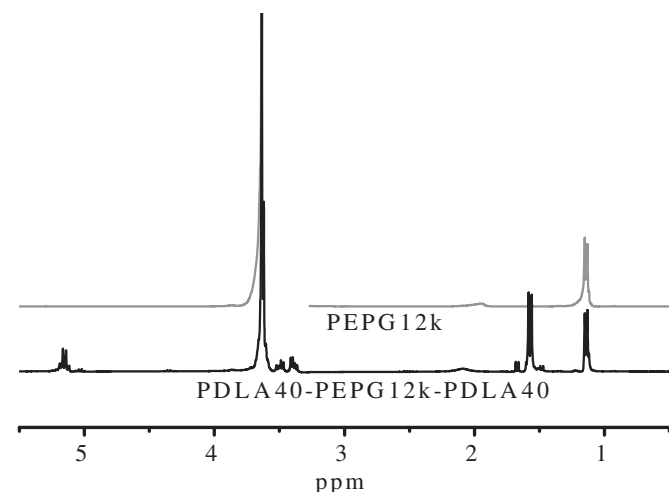


Fig. 1.  $^1\text{H}$  NMR spectra of PDLA40–PEPG12k–PDLA40 triblock copolymer.

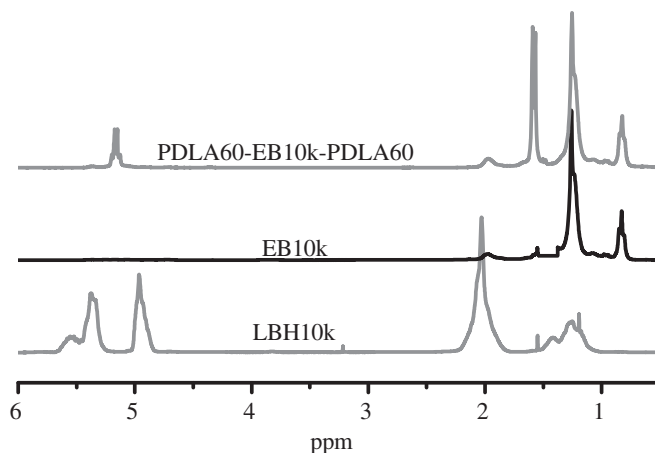


Fig. 2.  $^1\text{H}$  NMR spectra of LBH10k, EB10k and PDLA60–EB10k–PDLA60 triblock copolymer.

indicating conversion of unsaturated protons in the polymer to saturated protons ( $<1\%$  residual unsaturation). After polymerization the resonances from the methine protons ( $-\text{CH}$  quartet,  $\delta \sim 5.16\text{ ppm}$ ) and the methyl protons ( $\text{CH}_3$  doublet,  $\delta 1.57\text{ ppm}$ ) of the lactic acid repeat unit appear. The degree of polymerization was calculated using the integrated values for the methyl protons ( $-\text{CH}_3$  triplet,  $\delta 0.82\text{ ppm}$ ), from the erstwhile 1,2 vinyl repeat unit relative to the lactide repeat unit methine protons ( $-\text{CH}$  quartet,  $\delta \sim 5.16\text{ ppm}$ ). It was found to be in excellent agreement with the theoretical value. The dispersity values were 1.14, 1.10 and 1.17 for LBH10k, EB10k and PDLA60–EB10k–PDLA60, respectively. As the LBH10k midblock also contains minor amounts of monohydroxy terminated polybutadiene and polybutadiene without terminal hydroxyl groups, the triblock copolymer formed will contain small amounts of di-block copolymer and poly(ethylene–butylene) homopolymer. The slight broadening of the dispersity after polymerization may be due to the presence of these polymeric contaminants. The average molecular weights with respect to PS standards were  $18000\text{ g/mol}$  and  $26000\text{ g/mol}$  before and after polymerization, respectively.

##### 3.3. Properties obtained

The stress–strain curves and the composition of the PDLA40–PEPG12k–PDLA40 triblock based blends are shown in Fig. 3. The composition of the blends and the mechanical properties obtained are tabulated in Table 1. Neat PLA suffers from brittle fracture at a relatively low elongation at break ( $\sim 10\%$ ). It can be seen that, as the triblock content increases, the modulus decreases, and the strain at break increases indicating plasticization of the amorphous phase. The 50% blend, however, suffered fracture at a relatively low elongation. This is attributed to a matrix that consists mainly of the low molecular weight triblock copolymer, especially in high concentration.

For comparison, the stress–strain curves of the PDLA60–EB10k–PDLA60 midblock based blends are shown in Fig. 4. It can be seen that the mechanical properties of these blends (Table 2) are considerably different from the PEPG12k midblock based blends. The modulus is higher and the elongation at break is significantly lower than the PEPG midblock based blends (Fig. 3). For the 20% blend, a large variation in the elongation at break is observed, depending on the mode of failure. This is attributed to the presence of phase separated poly(ethylene–butylene) rich domains which can act as stress concentrators [6].

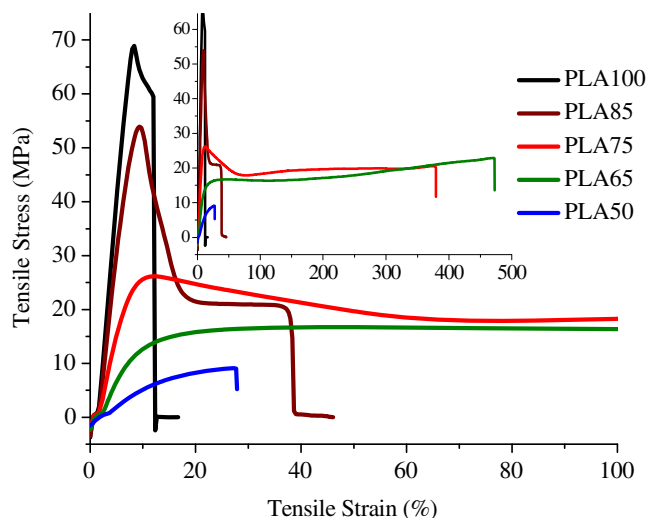


**Fig. 3.** Stress–strain curve for PDLA40–PEPG12k–PDLA40 triblock based blends (up to 100% strain). (Inset: significantly higher strain).

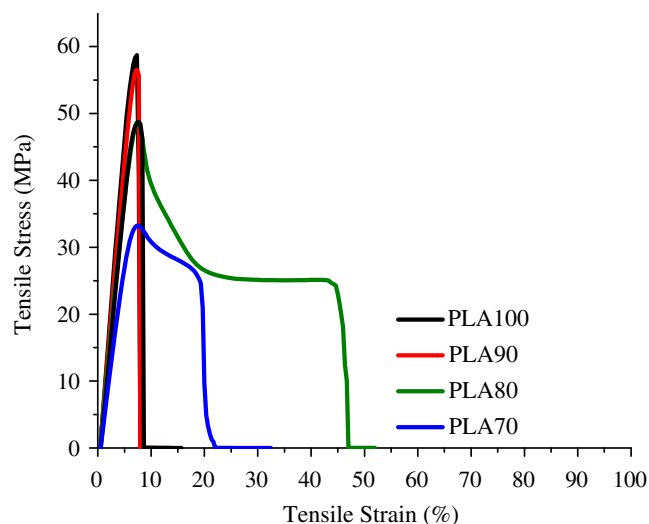


**Fig. 4.** Stress–strain curve for PDLA60–EB10k–PDLA60 triblock based blends.

### 3.4. Blend sample morphology

Undoubtedly the mechanical properties observed for the two types of samples need to be explained in terms of their morphological features. First, the extent of stereocomplex crystals formed needs to be analyzed. These crystals when present, effectively act as the reinforcement “particles”. In addition, it would be interesting to examine the nature of the amorphous phase, which must be a mixture of the uncrystallized triblock copolymer with PLLA. It is plausible that the details of morphology must then depend on the miscibility behavior of the triblock copolymers and PLLA, because the crystallization behavior depends on the local composition and chain dynamics.

To analyze the blend microstructure of the as-processed samples, ATR-IR was performed on the extruded dog-bone samples (Fig. 5). The band at  $\sim 909\text{ cm}^{-1}$ , assigned to the coupling of the C–C backbone stretching with  $\text{CH}_3$  rocking, is characteristic of the  $3_1$  helix associated with the stereocomplex, is present in all the samples with  $>15\%$  triblock copolymer. The presence of this band depends on both the crystallinity of the polymer and the type of helical conformation [10,11]. The infrared data obtained demonstrated that stereocomplex formation occurs during extrusion for both miscible and immiscible triblock copolymer/PLLA blends.

Thermal characterization was carried out in order to further examine the morphology of the two types of the as-processed samples. The DSC traces for the extruded-injection molded PDLA40–PEPG12k–PDLA40 triblock based blends are shown in Fig. 6A. The  $T_g$  of the blends initially is observed to decrease and then broaden with the increase in triblock content. The broadening of the  $T_g$  is completely consistent with the expected local

composition variations in this miscible PEPG based triblock/PLLA blend at high concentrations of the triblock copolymer [12,13]. The crystallization exotherm seen in Fig. 6B is associated with the crystallization of the stereocomplex crystals. In Fig. 6A, the exotherm and the subsequent endotherm at  $\sim 155\text{ }^\circ\text{C}$ , associated with crystallization and melting of the PLLA crystals, respectively, are virtually identical in value. A similar behavior is also observed for the second heating cycle. Therefore, the DSC data shows that stereocomplex crystals are formed under the processing conditions. In contrast, PLLA in this PEPG/PLLA blend remains amorphous and crystals are only formed during the heating cycle. In case of the 15% blend both stereocomplex and PLLA crystallization are found to occur during the DSC heating cycle because of the low PDLA content in this blend.

In addition, a theoretical calculation of the amount of each phase, and the predicted  $T_g$  of the amorphous phase, in this miscible blend is shown in Table 3. The amount of the triblock copolymer participating in the stereocomplex formation can be determined from the fraction of PDLA forming the stereocomplex crystals. This is determined from the melting enthalpy of the stereocomplex crystals in the DSC data. The theoretical stereocomplex content in the blend is twice the amount of PDLA in the blend, Table 3, column 2. The equation  $(\Delta H_{\text{stereocomplex}} / (2 \times \text{PDLA})) / 142$  summarizes the above procedure and gives the normalized stereocomplex degree of crystallinity (Table 3, column 3) [14]. The PEPG associated with this amount of the triblock copolymer (which participates in stereocomplex formation) is referred to as “bound PEPG” (column 5 = column 1  $\times$  column 3). The remaining triblock copolymer, and hence PEPG, referred to as “free PEPG”, will be dispersed in the amorphous phase, thus softening the amorphous phase. The “bound PEPG” is expected to be trapped within the amorphous regions of the stereocomplex crystal and may also contribute to the improvement in mechanical properties. The

**Table 1**  
Mechanical properties obtained for various samples.

Sample	%Triblock	%PEPG	%PDLA	%PLA	Modulus	Strain at
				2002D	(MPa)	break (%)
PLA 2002D	0	0	0	100	$1163 \pm 22$	$12 \pm 2$
85 PLA	15	10	5	85	$924 \pm 112$	$37 \pm 22$
75 PLA	25	17	8	75	$465 \pm 72$	$288 \pm 150$
65 PLA	35	24	11	65	$211 \pm 10$	$424 \pm 90$
50 PLA	50	34	16	50	$76 \pm 3$	$30 \pm 8$

**Table 2**  
Mechanical properties obtained for EB–PLA blends.

Sample	%Triblock	%EB	%PDLA	%PLA	Modulus	Strain at
				2002D	(MPa)	break (%)
PLA 2002D	0	0	0	100	$1012 \pm 7$	$7.8 \pm 0.7$
90 PLA	10	5	5	90	$930 \pm 10$	$7.4 \pm 0.2$
80 PLA	20	11	9	80	$834 \pm 39$	$26 \pm 24$
70 PLA	30	16	14	70	$664 \pm 83$	$24 \pm 6$

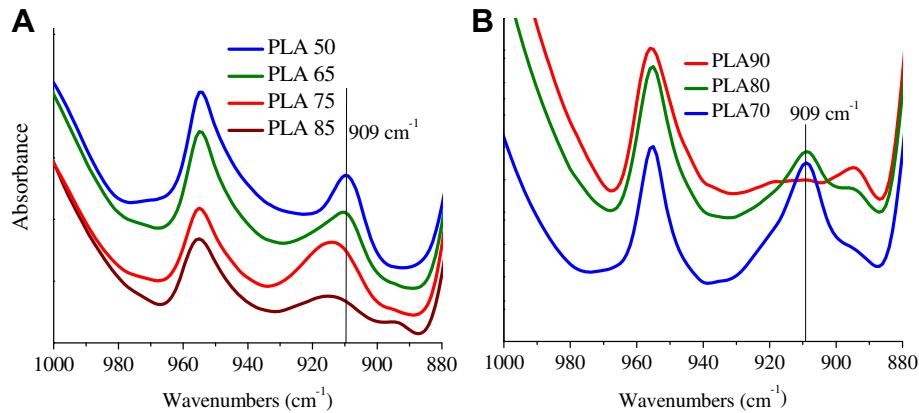


Fig. 5. Infrared spectra of triblock copolymer/PLLA blends; (A) PEPG12k midblock based blends; (B) EB midblock based blends.

amount of free PLLA is the total PLLA in the blend minus the PLLA involved in forming the stereocomplex ( $((\text{column } 4)/2)$ ). As the amount of free PLLA and free PEPG are known, the effective weight fraction of the two components in the continuous amorphous phase can be determined, and thus the  $T_g$  calculated using the Fox equation [5]. The  $T_g$  calculated are consistent with the observed drop in PEPG based triblock/PLLA blends up to 25% triblock content. For blends with higher triblock content a significant fraction of the triblock copolymer is present in the amorphous regions leading to variations in PEPG/PLLA local compositions. Thus the observed  $T_g$  is broader than the theoretically expected  $T_g$ .

The crystallization exotherm observed in the cooling cycle (Fig. 6B) can be assigned to the stereocomplex crystallization [15]. The typically low crystallization temperature is consistent with

other studies for the stereocomplex formation from the melt [11,15,16]. In case of the 15% blend, because of the low PDLA content, no stereocomplex crystallization occurs during the cooling cycle. In all the blends, PLLA does not crystallize during the cooling cycle, instead crystallizes during the second heating cycle (Fig. 6C). This observation is also consistent with previous observations [15]. However, the crystallization of PLLA, occurring at unusually lower temperatures, is directly related to the presence of the triblock copolymer and its plasticization effects [9]. The difference in the crystallization behavior of PLLA in the first and second heating cycle may be due to the restrictions introduced by different degree of stereocomplex crystallinity. We found the stereocomplex crystallinity is  $\sim 4\%$  lower for the sample at the end of the first cooling as compared to the as-processed sample. This small difference in the

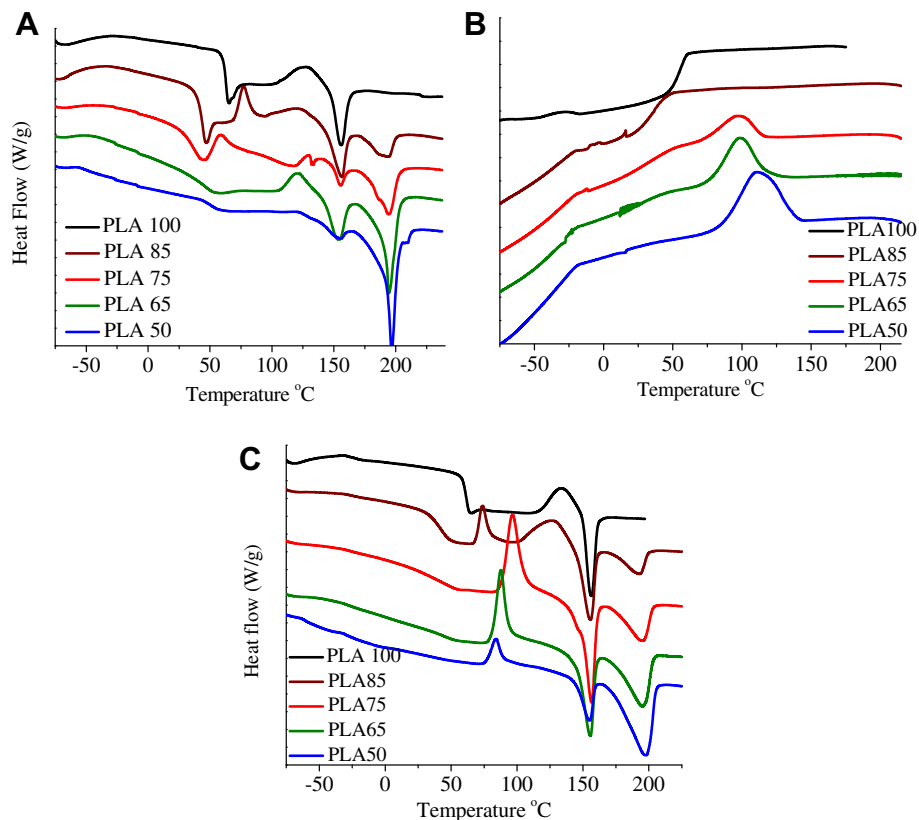


Fig. 6. DSC trace of the tensile specimens of PDLA40-PEPG12k-PDLA40 based blends. (A) First heating (20 °C/min), (B) first cooling (20 °C/min), (C) second heating (10 °C/min).

**Table 3**  
Phase and  $T_g$  calculation for PEPG12k midblock based blends.

Total PEPG (%)	Theoretical stereo-x (%)	Experimental stereo-x Xty	Experimental stereo-x (%)	% Bound PEPG	% Free PEPG	% Free PLLA	$T_g$ amorphous
<b>PLA75</b>							
17	16	40%	6.4	6.8	10	72	37°C
			Effective wt%		12	88	
<b>PLA 65</b>							
24	22	49%	10.8	11.8	12	60	29°C
			Effective wt%		17	83	

Stereo-x: stereocomplex; PEPG: poly(ethylene glycol-co-propylene glycol); Xty: crystallinity.

stereocomplex crystallinity may be significant in influencing the crystallization behavior of the amorphous matrix.

The DSC traces for the extruded-injection molded PDLA60–EB10k–PDLA60 triblock based blends are shown in Fig. 7A. In contrast to the PEPG/PLLA blends, there is no change in the glass transition temperature ( $\sim 55^\circ\text{C}$ ) of PLLA indicating an immiscible phase separated system. A  $T_g$  associated with the EB10k phase is found at  $\sim -58^\circ\text{C}$ . The stereocomplex melting enthalpy is seen to increase with increasing triblock content. The difference between enthalpy of PLLA crystallization and the melting enthalpy of PLLA is  $<3\text{ J/g}$ , indicating a very low degree of crystallinity of PLLA crystals in the as-processed samples. The degree of crystallinity of the stereocomplex crystals is  $\sim 46\text{--}53\%$  (Table 4) which is similar to the PEPG midblock blend system (Table 2). The calculation of the stereocomplex degree of crystallinity was performed using the same procedure as described in the PEPG midblock blend calculation. This shows that under the extrusion-injection molding processing condition, where thorough dispersion of the triblock copolymer in PLLA is achieved because of high shear,

stereocomplex crystallization occurs in both the miscible and immiscible midblock based blend.

The DSC measurements reveal a different picture for the PLLA phase in the two types of blends. In this case, unlike the PEPG/PLLA blend, it can be seen that very little crystallization occurs during the cooling cycle (Fig. 7B). The crystallization of the stereocomplex occurs in the subsequent heating cycle (Fig. 7C). No PLLA crystallization occurs in the heating cycle. A possible explanation is that the endothermal enthalpy of PLLA melting is compensated by the exothermal enthalpy of stereocomplex cold crystallization. The hindrance for stereocomplex formation during the cooling cycle is because of the phase separation of the triblock copolymer from PLLA in the melt. In the absence of high shear, the dispersion of the triblock copolymer in PLLA is poor, reducing contact between the PDLA and PLLA chains, thus slowing the rate of stereocomplex crystallization. This is in contrast to the PEPG midblock system (Fig. 6B), where the stereocomplex crystallization readily occurred during the cooling cycle. In that case, the PDLA chains are attached to PEPG triblock copolymers are miscible in the PLLA matrix, thus

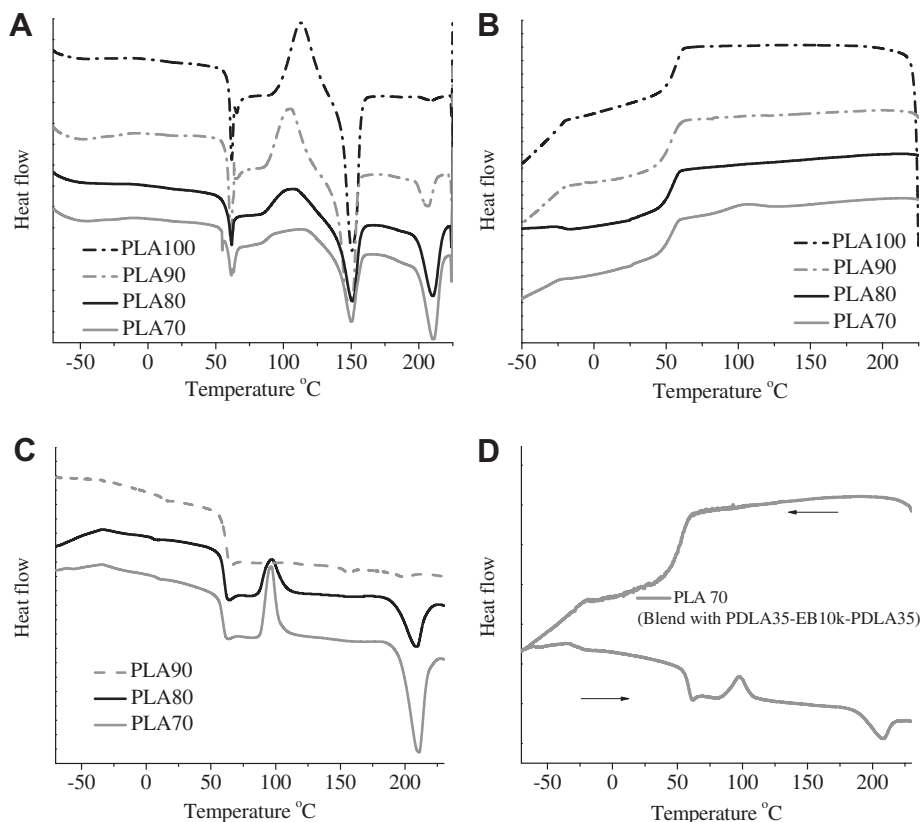


**Fig. 7.** DSC trace of the tensile specimens of PDLA60–EB10k–PDLA60 based blends (A) 1st heating (20 °C/min) (B) 1st cooling (20 °C/min) (C) 2nd heating (10 °C/min) (D) PLA70 (blend with PDLA35–EB10k–PDLA35) sample, first cooling (20 °C/min) and second heating (10 °C/min).

**Table 4**  
Calculation of stereocomplex degree of crystallinity in EB10k midblock blend.

Sample	%Triblock	% theoretical stereocomplex	dH (J/g)	norm dH (J/g)	Stereocomplex crystallinity (%)
PLA80	20	19	14	74	53
PLA70	30	28	18	64	46

facilitating the stereocomplex formation. To prove that the differences seen in the cooling cycle between the miscible and immiscible blends are not due to the difference in the degree of polymerization (DP) of the PDLA arm in the two triblock copolymers used (DP 60 vs DP 40), a blend with triblock copolymer PDLA35–EB10k–PDLA35 was studied. As shown in Fig. 7D no stereocomplex crystallization occurs in the cooling cycle in case of this blend.

From the analysis presented above, the two types of microstructure seen in the two types of blends are: 1. Stereocomplex crystals dispersed in a soft amorphous phase in the miscible PEPG midblock based blends. 2. Stereocomplex crystals dispersed in a glassy phase separated amorphous phase in case of the EB based immiscible midblock blends. The poly(ethylene–butylene) midblock based blends demonstrate that in order to obtain flexible tough materials, softening of the continuous amorphous phase is a necessary condition. However, these blends also exhibit some attractive properties such as the improved elongation at break.

### 3.5. Modeling of the two types of morphologies formed

In order to develop a better understanding of the effects of the midblock miscibility on the triblock copolymer/PLLA blend

crystallization behavior, and thus the resultant morphological features formed, an isothermal crystallization experiment was performed for both systems. Replication of the crystallization conditions that the blends experience in the extrusion/injection molding process (high shear force) is difficult. Hence, the isothermal crystallization experiment has a different thermal history as compared to the processed samples. The merit of this experiment is to enhance our understanding of the fundamental differences in the crystallization of the two blends, coupled with Raman mapping, enables assignment of the resultant morphological features formed. Fig. 8 shows the optical micrographs and Raman mapping of the miscible midblock based PLA75 blend in the melt and after isothermal crystallization. It can be seen that the triblock is miscible with PLLA in the melt (Fig. 8A). When crystallized isothermally at 155 °C (Fig. 8B) a substantially amorphous structure containing dispersed dendritic crystals is formed. This morphology is analyzed using the Raman mapping technique (Fig. 8C). Raman spectra have been obtained to establish the relative composition of each morphological feature. It has been established that the C=O stretching vibrations in the 1700 cm<sup>-1</sup> region are characteristic of each PLA crystalline form [10,17]. As it can be seen in Fig. 8C the crystalline regions show the distinguishing peaks of the PLA stereocomplex. PEPG exhibits broad features in the ~3100–2800 cm<sup>-1</sup> (CH<sub>3</sub> and CH<sub>2</sub> stretching) region. Raman spectra of the amorphous regions in the 3100–2800 cm<sup>-1</sup> region show contribution from PEPG, as well as, amorphous PLLA (Fig. 8C) proving the presence of the uncrystallized triblock copolymer along with amorphous PLLA in the continuous amorphous phase. These Raman data also support that the morphology in this PEPG based triblock/PLLA blend can be described as stereocomplex crystals dispersed in a soft continuous amorphous

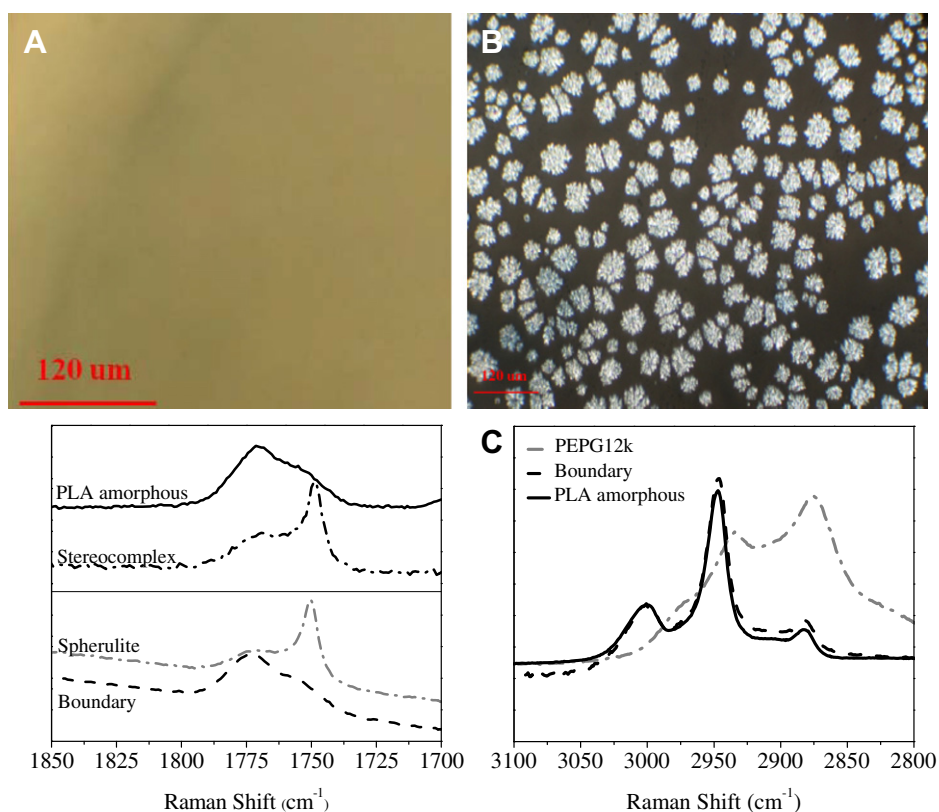


**Fig. 8.** (A) Optical micrograph of PLA75 in the melt at 220 °C, (B) polarized optical micrograph of PLA75 after completion of crystallization (isothermal crystallization 155 °C). (C) Raman mapping of the samples obtained by isothermal crystallization (left) 1850–1700 cm<sup>-1</sup>, (right) 3100–2800 cm<sup>-1</sup> regions.

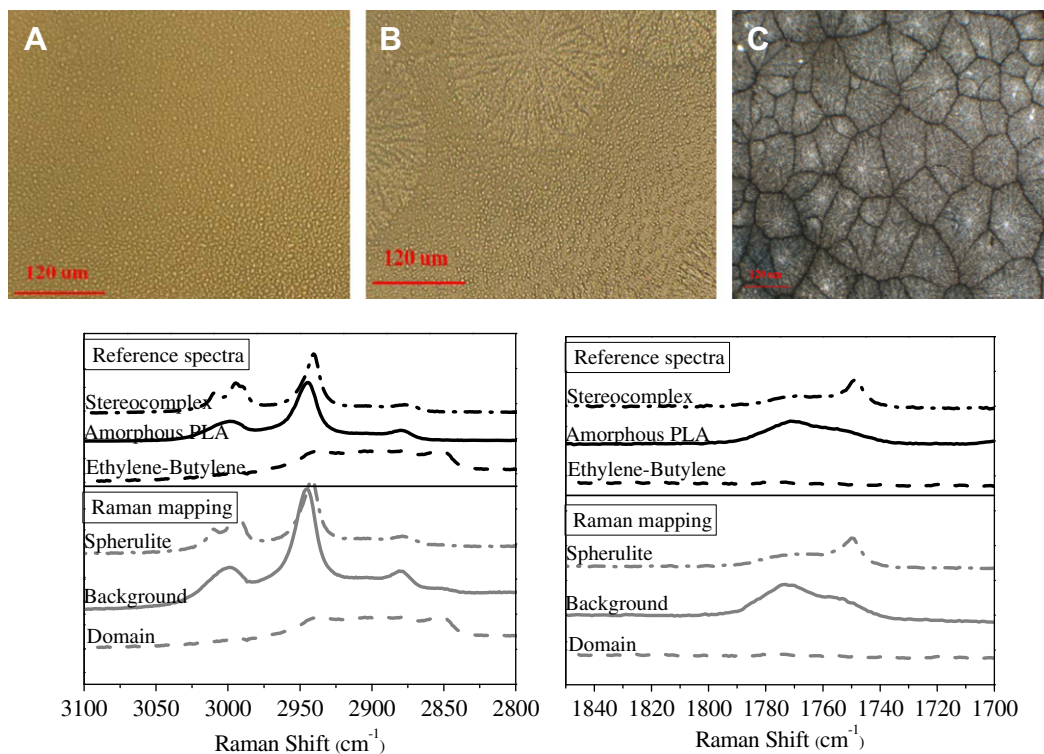


**Fig. 9.** (top) (A) Optical micrograph of PLA70 in the melt at 225 °C, (B) optical micrograph during isothermal crystallization at 155 °C, (C) polarized optical micrograph after completion of crystallization; (bottom) Raman mapping of the micrograph (B) at different points (1850–1700  $\text{cm}^{-1}$ , 3100–2800  $\text{cm}^{-1}$  regions) along with the reference spectra.

phase consisting of amorphous PLLA and the uncrystallized triblock copolymers.

The blend crystallization for the immiscible midblock based PLA70 blend is shown in Fig. 9. In the melt (Fig. 9A) at 225 °C a phase separated structure consisting of the poly(ethylene–butylene) rich domains (2–5  $\mu\text{m}$ ) dispersed in poly(lactic acid) is seen unlike the PEPG based triblock blends (Fig. 8A) where an isotropic melt was observed. Fig. 9B shows the morphology during the early stage of the crystallization process. The spherulites exhibit characteristic Raman active bands in the carbonyl ( $\sim 1760 \text{ cm}^{-1}$ ), as well as, the C–H stretching regions ( $\sim 2950 \text{ cm}^{-1}$ ) assignable to the stereocomplex crystals. The domains seen in the optical micrographs show characteristic bands for the poly(ethylene–butylene) copolymer while the background exhibits characteristic bands of amorphous PLA. These data show that the stereocomplex spherulites are growing in a phase separated melt consisting of droplets of the poly(ethylene–butylene) rich triblock copolymer in amorphous PLLA.

The isothermal crystallization experiments, along with the Raman mapping, clearly prove that an isotropic soft continuous amorphous, containing amorphous PLLA, and the uncrystallized triblock copolymer, are present in the case of the miscible midblock based blends. A phase separated amorphous phase containing poly(ethylene–butylene) rich domains in amorphous PLLA is present in the immiscible midblock based blends.

#### 4. Conclusions

Based on this study we can conclude that blends of stereocomplex forming triblock copolymers with PLLA provide access to a new morphology for toughening semicrystalline PLLA. This morphology can be described as stereocomplex crystals as nano-reinforcements, and a soft continuous amorphous phase as the stress absorbing component. Depending on the nature of the midblock in the triblock copolymer, different morphologies are

obtained. When the midblock is miscible with PLA, a soft continuous amorphous phase is formed, while in the case of an immiscible midblock, a glassy phase separated amorphous phase is obtained. The stereocomplex crystalline phase, however, is found to exist in both systems. Thus the dramatically different mechanical properties can only be explained in terms of the differences in the amorphous phase connecting the stereocomplex crystals. The most direct proof of the difference is seen in the DSC data. Because of the extensive mixing during extrusion, stereocomplex crystallization occurs in both types of triblock copolymer/PLLA blend systems. Further crystallization of PLLA is then hindered due to the reduced mobility resulting from the stereocomplex crystals formed. In the case of the miscible midblock (PEPG) based blends, the effective  $T_g$  of the PLLA is lowered in the amorphous phase because of the presence of the PEPG based triblock copolymers. In contrast, the  $T_g$  of PLLA remains unchanged due to the phase separated structures formed because of the immiscibility of the EB based triblock copolymer/PLLA blend. In the subsequent heating and cooling cycles, the rate of stereocomplex crystallization was found to be slower in the immiscible midblock based blends, in comparison to, the miscible midblock based blends. In all cases, the PEPG midblock based blends were found to have very high elongation, at break and low modulus, indicating plasticization was the dominant toughening mechanism. The poly(ethylene–butylene) midblock based blends exhibited high modulus and low elongation indicating rubber toughening was the dominant toughening mechanism. These stereocomplex forming triblock copolymers provide access to develop tough yet flexible semicrystalline poly(lactic acid) based blends.

#### References

- [1] Smith PB, Leugers A, Kang SH, Yang XZ, Hsu SL. *Macromol Symp* 2001;175: 81–94.
- [2] Rathi SR, Chen X, Coughlin EB, Hsu SL, Golub C, Tzivanis M. *Polymer* 2011; 52(19):4184–8.



- [3] Pillin I, Montrelay N, Grohens Y. *Polymer* 2006;47(13):4676–82.
- [4] Desai S, Thakore IM, Sarawade BD, Devi S. *Eur Polym J* 2000;36(4):711–25.
- [5] Fox TG. *Bull Am Phys Soc* 1956;1:23.
- [6] Ishida S, Nagasaki R, Chino K, Dong T, Inoue Y. *J Appl Polym Sci* 2009;113(1):558–66.
- [7] Lin SY, Lee CJ, Lin YY. *Pharm Res* 1991;8(9):1137–43.
- [8] Ran XH, Jia ZY, Han CY, Yang YM, Dong LS. *J Appl Polym Sci* 2010;116(4):2050–7.
- [9] Jia ZY, Tan JJ, Han CY, Yang YN, Dong LS. *J Appl Polym Sci* 2009;114(2):1105–17.
- [10] Kister G, Cassanas G, Vert M. *Polymer* 1998;39(2):267–73.
- [11] Sun JR, Yu HY, Zhuang XL, Chen XS, Jing XB. *J Phys Chem B* 2011;115(12):2864–9.
- [12] Lodge TP, McLeish TCB. *Macromolecules* 2000;33(14):5278–84.
- [13] Savin DA, Larson AM, Lodge TP. *J Polym Sci Pt B – Polym Phys* 2004;42(7):1155–63.
- [14] Anderson KS, Hillmyer MA. *Polymer* 2006;47(6):2030–5.
- [15] He Y, Xu Y, Wei J, Fan ZY, Li SM. *Polymer* 2008;49(26):5670–5.
- [16] Yamane H, Sasai K. *Polymer* 2003;44(8):2569–75.
- [17] Aou K, Hsu SL. *Macromolecules* 2006;39:3337–44.